Available online at www.sciencedirect.com
ScienceDirect
Optics Communications 280 (2007) 103–109
OPTICS COMMUNICATIONS
www.elsevier.com/locate/optcom

Infrared and visible spectroscopic studies of the ytterbium doped borate $Li_6Y(BO_3)_3$

J. Sablayrolles [a], V. Jubera [a,*], F. Guillen [a], R. Decourt [a], M. Couzi [b], J.P. Chaminade [a], A. Garcia [a]

[a] *ICMCB-CNRS, Université Bordeaux 1, 87 Avenue Dr. A. Schweitzer, 33608 Pessac Cedex, France*
[b] *Groupe de Spectroscopie Moléculaire (GSM), Institut des Sciences Moléculaires (ISM), UMR 5255, CNRS-Université Bordeaux 1, 33405 Talence Cedex, France*

Received 10 May 2007; received in revised form 19 July 2007; accepted 30 July 2007

Abstract

The spectroscopic study of trivalent ytterbium doped $Li_6Y(BO_3)_3$ is conducted in the UV–visible and infrared range. An excitation in the charge transfer band of ytterbium has been selected in order to reduce the reabsorption effect on the IR emission intensity. The maximum of the emission is located at 972 nm for an excitation at 230 nm. The energy level assignment has been successfully conducted using vibrational spectroscopy to distinguish the pure electronic transitions from the phonon-assisted ones. The splitting of the $^2F_{5/2}$ and $^2F_{7/2}$ components is equal to 523 cm^{-1} and 676 cm^{-1}, respectively. The decay time dependence as a function of the concentration is also reported. The calculated value τ_{rad} is about (1.03 ± 0.01) ms for the 1% doped material. For the highest concentration, an IR excitation gives rise to the observation of a blue-green luminescence caused by two mechanisms: an erbium emission at 550 nm after upconversion and a cooperative luminescence of ytterbium ions.

Keywords: Ytterbium; Borate; Infrared luminescence; Upconversion; Cooperative emission

1. Introduction

The infrared emission between 4f levels of the ytterbium ion is studied in many compounds because of its applications in all-solid-state lasers operating in a continuous or pulsed fashion (non-exhaustive list [1–7]). The laser effect, obtained by stimulated emission is depending a lot on spectroscopic properties. Their knowledge can help to predict the potentiality of a material doped with ytterbium. First, the crystal field has a direct impact on the broadening of the spectral lines; it induces a splitting of the Stark components that can results in a larger emission range of the ytterbium. A strong electron–phonon coupling also enlarges the electronic lines. The attribution of the electronic transitions between Stark levels using absorption and emission spectra is not so trivial. This ion possesses only two spectroscopic terms ($^2F_{7/2}$ for the ground state and $^2F_{5/2}$ for the excited state) split by the crystal field in 4 and 3 Stark levels, respectively. The weak strength of this perturbation leads to levels separated by only several hundreds of cm^{-1}. This is why at room temperature the Stark levels are thermally populated increasing the number of electronic transitions on absorption and emission spectra. Moreover, the ytterbium ion gives rise to vibronic transitions due to its high electron–phonon coupling [8]. The energy level attribution can be verified by a method called the barycenter plot [9]. To generate ultrashort pulses, the laser crystal has to amplify broad emission spectra. A laser amplification requires also the knowledge of the possible excited levels which must be at higher energy than the laser transition: reabsorption of the infrared fluorescence is generally observed due to the proximity between absorption and emission lines. Upcon-

* Corresponding author. Tel.: +33 5 40 00 37 03; fax: +33 5 40 00 27 61.
E-mail address: jubera@icmcb-bordeaux.cnrs.fr (V. Jubera).

0030-4018/$ - see front matter © 2007 Elsevier B.V. All rights reserved.
doi:10.1016/j.optcom.2007.07.034

version processes of impurities and concentration quenching of the activator have to be avoided to obtain good laser efficiency. Moreover, the laser application requires good compatibility between the absorption spectra of the materials and the emission of the commercial high power laser diodes. Finally, the decay time of the emission is an important parameter as it is directly related with the facility to create the inversion. Considering the single crystals, physical parameters like the thermal conductivity must be determined to prevent the lack of stability or efficiency and deterioration of the laser materials.

The $Li_6Y(BO_3)_3$ host lattice has early be considered as a good candidate for laser applications. Since 1989, articles have been published on the spectroscopic characteristic of Nd^{3+} doped $Li_6Y(BO_3)_3$ [10–13]. Latter several spectroscopic studies were performed using trivalent europium [14–17] or cerium [18–20] as dopants in order to use this borate as a red phosphor for visualization or as scintillator for the detection of neutrons, respectively. Some articles also report the luminescence of trivalent erbium [21,22]. We recently mentioned the laser performance in continuous, mode-locked and Q-switch modes of $Li_6Y(BO_3)_3:Yb^{3+}$ also called LYB crystals [5,7]. A first attribution of the Stark components of an Yb-doped LYB crystal was proposed by Brenier et al. [6]. In this work, we complete this study on powders materials for an excitation in the charge transfer band of ytterbium in order to avoid the reabsorption phenomena and, by using vibrational spectroscopy and calculation to discriminate the pure electronic transition from the phonon-assisted ones. We also report for the highest concentration in ytterbium, a blue-green luminescence for an excitation at 932 nm in the IR levels which can be deleterious phenomena for laser efficiency.

2. Experiments

2.1. Sample preparation

Polycrystalline powders of $Li_6Y(BO_3)_3:Yb^{3+}$ were synthesized by solid-state reaction at 750 °C [5]. High purity ($\geqslant$99.99%) rare earth oxides were used to obtain several ytterbium concentration: 1%, 2%, 5%, 10%, 20%, 50% and 100% of molar substitution rate. Purity of final products was checked by XRD.

A crystal of $Li_6Y(BO_3)_3$ doped with 15% of ytterbium was grown by the Czochralski method [5]. Ytterbium concentration in the crystal was determined by microprobe analysis. For absorption measurements, a plate of 4.5 mm × 4.5 mm × 2.45 mm was optically polished. This crystal will be used to obtain the absorption spectra of ytterbium in the $Li_6Y(BO_3)_3$ matrix.

2.2. Experimental setup

Absorption spectra were recorded by transmission using a double beam spectrophotometer (CARY 5000 UV–VIS-NIR) between 800 nm and 1200 nm.

The emission spectra were recorded using a spectrofluorimeter (Edinburgh Instruments FL 900 CDT) with a M30 monochromator connected to a germanium AD403L detector for infrared emission and a PM Hamamatsu R955 for visible detection. A Xe lamp or a laser diode was used as excitation source.

The low temperature measurements of the absorption and emission spectra were recorded on the same spectrometers equipment with an optistat Oxford Instrument cryostat cooled by a liquid helium circulation.

Infrared lifetimes measurements were performed with a digital oscilloscope (LeCroy Waverunner LT 342) equipped with a germanium AD403HS detector coupled to a HR640 monochormator (Horiba Jobin-Yvon). All of these were piloted by a home-made LabView program.

Visible lifetimes were recorded on an intensified CCD camera (Andor Technology). The excitation source for both measurements was an OPO (GWU355SH) pumped with a YAG:Nd 10 Hz continuum Surelite.

Raman spectra of borate groups were performed on a Raman spectrometer (LabRam Dilor) equipped with a CCD detector and connected to an Ar laser source (spectra physics 2030 model), which emits at 514.5 nm.

3. Results and discussion

3.1. Assignment of Yb^{3+} energy levels

A first level attribution was made by Brenier et al. [6] on a single crystal doped with ytterbium. The level assignment is realized from a low temperature spectrum using an infrared source for emission spectrum. The originality of our work is to compare the low temperature spectrum to Raman spectrum in order to identify purely electronic from vibronic lines and to calculate and to compare the theoretical positions of the different transitions with the experimental pattern. Another noteworthy fact is that in our case, the samples are polycrystalline powders and an excitation in the ultraviolet range through the charge transfer state of the dopant was preferred. The two 4f levels of the ytterbium ion are split by the crystal field in four Stark levels for the ground state $^2F_{7/2}$ and three for the excited state $^2F_{5/2}$. These levels will be labeled from 1 to 4 for the ground state and 5–7 for the excited state, the 1 level being the ground state and the 7 level, the highest energy component (see the identification in Table 1 or the inset of Fig. 1).

At room temperature, the absorption and emission spectra are too complicated to be correctly interpreted. Because of the thermal distribution of electrons population, a maximum of 12 pure electronic transitions which correspond to the radiative de-excitation from the three components of the $^2F_{5/2}$ level on the four components of the $^2F_{7/2}$ level are expected. This can be limited by low temperature measurements. In Fig. 1, the absorption spectra were recorded on the crystal plate with unpolarized light at room and low temperature. Three main peaks are observed at 972 nm,

Table 1
Energy levels of ytterbium doped $Li_6Y(BO_3)_3$ obtained for $Li_6Y(BO_3)_3$:Yb 1%.

Identification of the Stark components		Energy (cm^{-1})
$^2F_{5/2}$	7☆	10811
	6 △	10482
	5 □	10288
$^2F_{7/2}$	4★	676
	3 •	507
	2 ▲	367
	1 ■	0

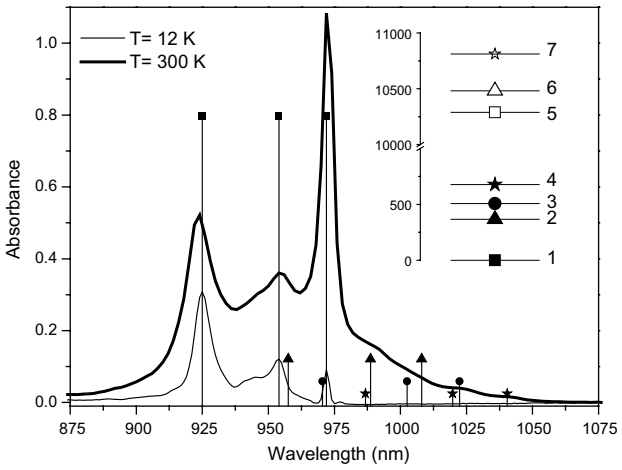

Fig. 1. Absorbance spectra at 12 K and room temperature (thin and bold line, respectively) of $Li_6Y(BO_3)_3$:Yb 1% with position of theoretical absorption lines (vertical lines). The symbols at the top of the vertical lines indicate the levels from which the absorption occurs (black square: level 1, black triangle: level 2, black circle: level 3, black star: level 4). Inset: energy scheme.

954 nm and 925 nm, respectively. At low temperature, these lines are thinner and they correspond mainly to transitions from the level 1 to the upper levels 5–7. In Fig. 2, the emission of the 1%-doped sample was recorded under excitation in the charge transfer state at 230 nm [23]. At low temperature four lines are peaking at 972 nm, 1008 nm, 1022 nm and 1040 nm, respectively.

Note: The very strong absorption of the excitation beam at 230 nm ensures a small penetration of the excitation beam in the sample and by the way, the emission of the surface is less affected by reabsorption like radiation trapping. Fig. 3 shows the modification observed on emission spectra of a high doped ytterbium sample (molar substitution of 20%) excited either in the charge transfer state or in the level $^2F_{5/2}$. This high concentration has been chosen to make clearer the reabsorption effect on this matrix. The spectra have been normalized to the area under the curve in order to compare them. It is clear that in the case of an excitation in the infrared level, the emission spectrum is strongly affected by radiation trapping, leading to a weak emission of the most energetic lines (short wavelengths) and an over emission intensity at 1040 nm. The emission

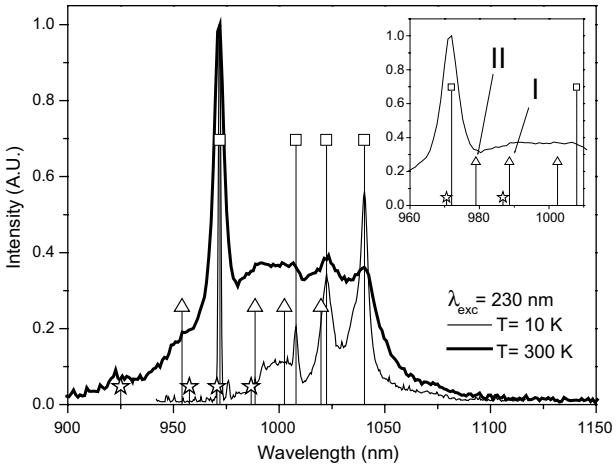

Fig. 2. Emission spectra at 10 K and room temperature (thin and bold line, respectively) of $Li_6Y(BO_3)_3$:Yb 1% for an excitation at 230 nm with position of theoretical emission lines (vertical lines). The symbols at the top of the vertical lines indicate the levels from which the emission occurs (empty square: level 5, empty triangle: level 6, empty star: level 7). Inset: Hypothetical positions I and II for $6 \rightarrow 2$ transition.

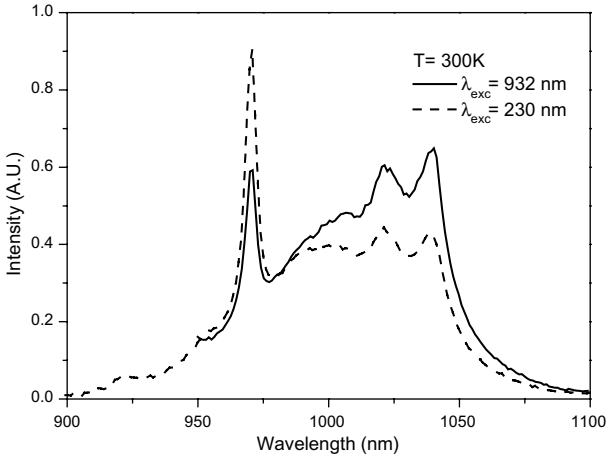

Fig. 3. Normalized emission spectra of $Li_6Y(BO_3)_3$:Yb 20% (area) at room temperature excited at 230 nm (broken line) and 932 nm (solid line).

spectrum under ultraviolet excitation shows a strong line at 972 nm followed by a constant emission intensity. This observation puts in evidence the strong modification of the emission spectrum for an excitation in the IR compared to the spectrum obtained for an excitation in the ultraviolet and validates our approach to obtain a better intensity ratio of the emission lines by using an excitation in the charge transfer state. This is mainly due to higher absorption coefficient of the charge transfer state in the ultraviolet than the absorption coefficient of the 4f–4f lines in the infrared.

However, the four emission lines previously pointed in Fig. 2 cannot be attributed unambiguously to Stark levels without checking with Raman spectrum. As they can be replicas of electronic transitions by phonons coupling, a strong interaction of the ytterbium ion with lattice vibra-

tions must be considered [8]. This electron–phonon coupling results in additional vibronic transitions in the spectra. To discriminate the electronic transitions from vibronic ones (non-pure electronic transitions), the low temperature emission and absorption spectra already reported in Figs. 1 and 2 are compared to the Raman spectrum. In Fig. 4, the spectra are plotted in wave number from an origin set on the 1–5 zero-phonon transition for absorption and emission spectra and the Rayleigh line of the Ar laser (514.5 nm) used to record the Raman spectrum. First of all the $1 \rightarrow 5$ line also called zero-phonon line is attributed to the common line of absorption and emission spectra at low temperature. This strong line is located at 972 nm (10,288 cm^{-1}). In Fig. 4, looking at the emission spectrum, the attribution of emission transitions from the lowest level of the excited state 5 to the three levels 2–4 of the ground state seems obvious as the three main peaks of the low temperature emission spectrum do not overlap with any vibronic states (no Raman vibration are detected on those positions). Regarding the absorption spectra in Fig. 4 the same observation can be made for the $1 \rightarrow 7$ transition of the absorption spectrum which corresponds to the highest energy transition. However by taking into account these data, the attribution of the $1 \rightarrow 6$ transition is not so obvious. A stage is observed on the emission and absorption spectra, in the range 150–350 cm^{-1} over the $1 \rightarrow 5$ transition and it corresponds to several Raman transitions. This is why the absorption line observed at 196 cm^{-1} above the $1 \rightarrow 5$ transition (labeled position I) cannot be simply attributed to the $1 \rightarrow 6$ transition. As a matter of fact, this transition could also be assigned at the value 294 cm^{-1} above the $1 \rightarrow 5$ transition and named position II on the graph. In order to discriminate between these two possibilities and by considering the criteria obtained with the emission from the level 5, a simulation of the position of all the transitions from excited

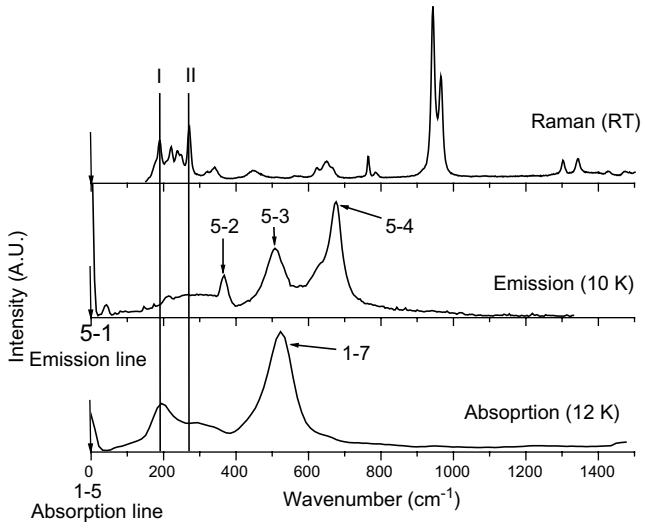

Fig. 4. Room temperature Raman (A_g vibration modes) spectra ($\lambda_{exc} = 514.5$ nm) and low temperature absorption and emission spectra ($\lambda_{exc} = 230$ nm) for Yb^{3+} electronic transitions attribution.

state to ground state has been conducted considering the two possible 6 level positions. The result was compared to the room temperature emission spectrum. The more significant part is represented in the inset in Fig. 2. By doing so, a noteworthy fact is that the hypothetic transition $6 \rightarrow 2$ occurs at 979 nm (10,215 cm^{-1}) for the level 6 correlated with the position II, and no shoulder is detected on room temperature spectrum. However, position I of the level 6 gives rise to a $6 \rightarrow 2$ transition at 989 nm (10 115 cm^{-1}) where emission intensity is actually observed. By consequence, the position I was attributed to the $6 \rightarrow 2$ transition even if it is probably not a purely electronic transition. Finally the energy scheme is resumed in Table 1. In Figs. 1 and 2 all the transitions are plotted for both absorption and emission spectra by vertical lines (the symbol at the top of the vertical line indicates the level responsible of the absorption or emission line, see Table 1) with intensity proportional to the thermal distribution (f_i) of each Stark level i following this equation:

$$f_i = \frac{\exp\left(\frac{E_0 - E_i}{kT}\right)}{\sum_i \exp\left(\frac{E_0 - E_i}{kT}\right)} \quad (1)$$

where E_0 is the energy of the lowest Stark level of the 4f state considered ($E_0 = 0\ cm^{-1}$ for levels 1–4 and 10,288 cm^{-1} for levels 5–7), E_i is the energy of the Stark level i, k the Boltzmann constant and T the temperature.

The attribution of the transitions lines and the energy positions of the different Stark component described here are close to the one found by Brenier et al. [6]. However, the position of the level 2 has been revised. The authors fixed it at 253 cm^{-1}. As a matter of fact, this position has been excluded because it corresponds to Raman transitions and we positioned the level 2 at 367 cm^{-1} above the level 1. The same authors observed, on the single crystals, two ytterbium emissions at low temperature which can be associated to two $5 \rightarrow 1$ transitions and the first hypothesis made for the second ytterbium environment is a substitution of the Li^+ ions with charge compensation. The structure of the $Li_6Y(BO_3)_3$ possesses a unique independent crystallographic site for the rare earth, the polyhedron YO_8, which offers one preferential substitution site for the ytterbium ion as the cationic size are very closed ($rY^{3+} = 1.019$ Å and $rYb^{3+} = 0.985$ Å) [24]. Previous investigations performed on the luminescence of trivalent europium ($rEu^{3+} = 1.067$) in the yttrium phase, revealed that the europium is located in an unique rare earth polyhydron [25,26]. In the pure ytterbium phase, the average distance between Yb^{3+} and O^{2-} is equal to 2.351 Å [27]. In this unit cell, the lithium ions are fourfold or fivefold coordinated with the oxygen atoms and the average distances d_{Li-O} in the polyhedra vary from 1.899 Å to 2.105 Å [27]. These cationic environments are too small to imagine a substitution of the lithium by the europium. In 1982, Kbala et al. [28] published that it is possible to substitute a pair of $Li^+ - Y^{3+}$ atoms by a tetravalent cation which results in a ionic conductivity of the matrix. This means that the structure can

accept small local disorder. Another hypothesis to explain this second zero-phonon line is that the compound presents a deficit in lithium ions mainly due to the way of the temperature synthesis that can favor the departure of the lightest ions. The compensation charge can be assumed by an oxygen vacancy as we clearly do not have tetravalent ion in our case. This might result in a local reorganization of the anions and a new ytterbium environment. In our sample, a small emission line is also observed at 976 nm at low temperature. In the present work, the spectroscopy was performed on powders. A very small transition can be distinguish at the bottom of the $5 \rightarrow 1$ line at low temperature (Fig. 2) but no more characterization was performed on this second-type emission because of its weak intensity. This transition can also be associated in the present situation (characterization on polycrystalline sample and not on single crystal) to the zero line transition (line $5 \rightarrow 1$) of small quantities of impurities as Y_2O_3:Yb^{3+}. Investigations are still going on to determine what the environment of the second-type ytterbium is.

The barycenter of each 4f level has been calculated and compared to the barycenter plot method introduced by Antic-Fidancev [9] (Fig. 5). This method is based on the fact that the spin orbit splitting of the two 4f levels of the ytterbium is host independent. Taking the lowest level of the ground state as the energy origin, the barycenter of the $^2F_{5/2}$ level is then linearly dependent to the one of the level $^2F_{7/2}$ and follow the semi-empiric equation $y = 10{,}180 + 0.95x$ [29–31]. The energy level attribution is confirmed by the proximity of the barycenter plot to the theoretical line. Other lattices are reported on this diagram for comparison.

3.2. Lifetime study

Lifetime measurements have been conducted for each concentration of ytterbium under excitation in the highest level of the excited state ($1 \rightarrow 7$ transition) at 925 nm and for three different emission wavelengths. The results which correspond to the $5 \rightarrow 1$, $5 \rightarrow 4$ and $7 \rightarrow 4$ transitions are plotted in Fig. 6. All these transitions are associated to the main emission previously described. The advantage of the setup used is that the lifetimes were recorded across all the emission spectrum. It allows a really good accuracy of the measurements. Each value can be estimated at more or less 1%. It is then possible to discriminate the values for different initial Stark levels, as long as they are not superimposed on the emission spectrum, and to compare them. All the lifetimes measured were fitted with a single exponential decay as the studied emission spectra in concentration are related to the ytterbium ion located in the unique yttrium crystallographic site. The calculations were made for transitions from level 5 to the Stark levels 1 and 4. The corresponding transitions are peaking at 972 nm and 1040 nm, respectively. For the $5 \rightarrow 1$ transition at 972 nm lifetimes are systematically shorter than for the $5 \rightarrow 4$ transition at 1040 nm: considering the assignment of the transitions in Fig. 2, two transitions ($5 \rightarrow 1$ and $7 \rightarrow 3$), occur at 972 nm. The fit of the experimental curve was performed using the contribution of the two considered transitions. The lifetime of level 7 was measured at 987 nm ($7 \rightarrow 4$ transition) for all compositions and it was found to be systematically lower than the one of the transition $5 \rightarrow 4$ (Fig. 6). The thermal distribution of level $^2F_{5/2}$ population can be calculated using the Boltzmann statistics following Eq. (1). This calculation gives a fraction of 5% on level 7 at room temperature; this contribution to the emission spectrum could decrease the observed lifetime. No particular fact was observed on lifetime corresponding to transitions from level 6, probably because it is of the same order of magnitude of level 5.

The classical increase due to reabsorption [32] is observed until a substitution rate of 10% for transitions from level 5 to level 4. As a matter of fact, the overlap between absorption and emission spectra allow radiative

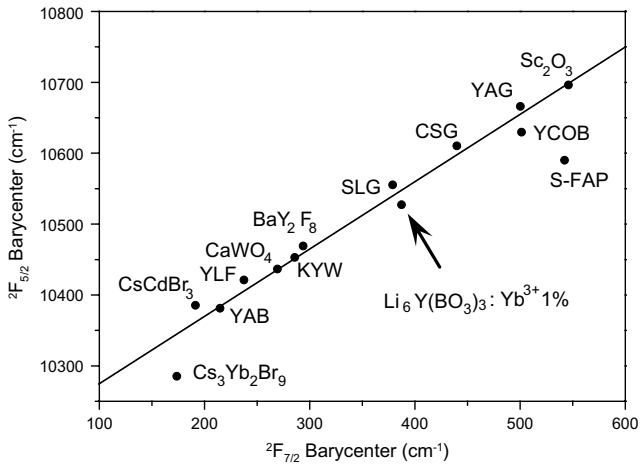

Fig. 5. Barycenter plot for various Yb^{3+}-doped materials indicating the position of the $Li_6Y(BO_3)_3$:Yb 1%.

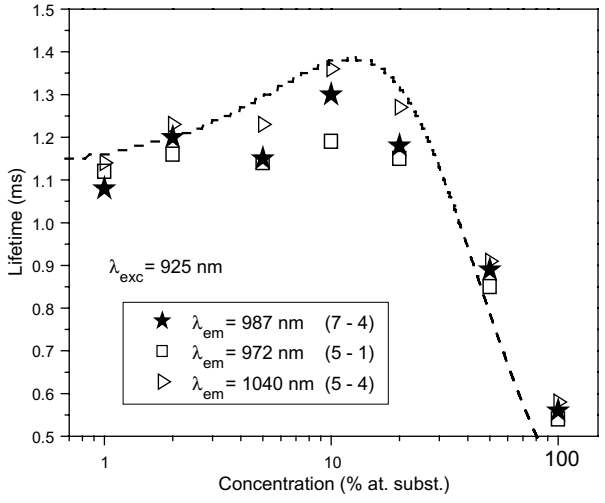

Fig. 6. Decay times dependence versus ytterbium concentration at room temperature ($\lambda_{exc} = 925$ nm). Broken line: theoretical fit.

reabsorption. A study made by Milne [33] on a gas medium but transposable to solid-state materials, showed that such increase should be observed for the diffusion of a radiation along a propagation direction. From 10% of substitution to the phase $Li_6Yb(BO_3)_3$ (100% of substitution) the lifetime decreases down to 540 μs. This strong diminution of the lifetime is the result of the concentration quenching [34,35]. As a matter of fact, when the concentration increases, the distance between ytterbium ions decreases and resonant transfers can occur, resulting in an energy migration. This energy is either released by spontaneous emission either quenched by a defect or an impurity in the lattice (which is the more probable case when concentration increases). Finally this quenching mechanism shortens the lifetime.

Moreover, it is possible to calculate a theoretical value of the lifetime from the reciprocity relations introduced by MacCumber [36] for transitions with overlap between absorption and emission:

$$\frac{1}{\tau_{\text{rad}}} = \frac{g_f}{g_i}\frac{8\pi n^2 c}{\bar{\lambda}^4}\int \sigma_{\text{abs}}(\lambda)\mathrm{d}\lambda$$

where g_f and g_i are the degeneracy of final and initial levels (respectively $^2F_{5/2}$, $g_i = 6$ and $^2F_{7/2}$, $g_f = 8$), n the refractive index, c the light velocity, $\bar{\lambda}$ the emission median wavelength (1003 nm calculated from the integration of emission spectrum) and σ_{abs} the absorption cross-section. It gives a calculated value of $\tau_{\text{rad}} = 1.03$ ms shorter than the one found for the lowest concentration of ytterbium measured (molar substitution of 1% by Yb^{3+}), probably because reabsorption already occurs and lengthens the lifetime.

A recent model [32] based on the Milne's approach of radiation trapping was developed to interpret concentration quenching processes in ytterbium doped sesquioxydes. This model takes into account either a fast diffusion towards intrinsic defects or a limited diffusion process, the quenching probability being of the same order as the transfer probability. This particular case can be simply explained by the high probability of resonant transfers between the ytterbium ion and other rare earths (such as erbium). It has been observed that the limited diffusion process fits better experimental data [32,37,38]. Because we also observed the presence of impurities, we chose to apply here this last model. This model links the lifetime τ as a function of the ion concentration N (in ions/cm^3):

$$\tau(N) = \frac{\tau_w(1+\sigma N l)}{1+(9/2\pi)(N/N_0)^2}$$

where τ_w the radiative lifetime at weak concentration, σ the transition cross-section, l the optical path in the sample, N_0 the critical concentration.

The calculus has been conducted using τ_w, σl and N_0 as variables. The fit of the experimental acquisitions (see pointed line in Fig. 6) has been conducted for the emissions from level 5 with the following parameters: $\tau_w = 1.12$ ms, $\sigma l = 7.2\times10^{-22}$ cm^3 and $N_0 = 1.8\times10^{21}$ ions/cm^3. The value of τ_w is close to the value of τ_{rad} calculated above which is coherent as τ_w represents the lifetime without radiation trapping effect. The value of N_0 (the self-quenching parameter) is lower than that found for CaF_2:Yb^{3+} ($N_0 = 7.47\times10^{21}$ ions/cm^3) [38], Y_2O_3:Yb^{3+} ($N_0 = 1.9\times10^{21}$ ions/cm^3) [32] and YAG:Yb^{3+} ($N_0 = 2.3\times10^{21}$ ions/cm^3) [37] a drawback meaning that the tendency of the material to be self-quenched is higher.

3.3. Blue-green luminescence

The luminescence in the visible range was studied under diode excitation at 932 nm. We chose to present here the result obtained for a high concentration in order to obtain good emission intensity. Fig. 7 shows lines peaking at 550 nm and a large band centered at 500 nm. By consequence, two processes were identified on the 20% doped sample emission spectrum (Fig. 7): presence of impurities of Er^{3+} and cooperative luminescence. These emissions have been studied in several other lattices [38–40]. The concentration of erbium impurity is 5 ppm from the purity certificate of the raw material Yb_2O_3. Energy transfer from Yb^{3+} to Er^{3+} (transitions $^4I_{15/2} \rightarrow {}^4I_{11/2}$ followed by $^4I_{11/2} \rightarrow {}^4F_{7/2}$) and two photons upconversion leads to emissions in the green (transitions $^4S_{3/2} \rightarrow {}^4I_{15/2}$) and in the red range (transitions $^4F_{9/2} \rightarrow {}^4I_{15/2}$). The other luminescence centered at 500 nm is attributed to cooperative luminescence, that is to say simultaneous de-excitation of two neighbor ytterbium ions giving rise to an emission from a virtual level located at about 20,000 cm^{-1}. This emission was observed for the first time by Nakazawa in $YbPO_4$ [41] and Ovsyankin [42] showed that a good approximation of this spectrum is given by the convolution product of the infrared spectrum:

$$G(2\bar{\nu}) = \int F(\bar{\nu})F(\bar{\nu}-\bar{\nu}')\mathrm{d}\bar{\nu}'$$

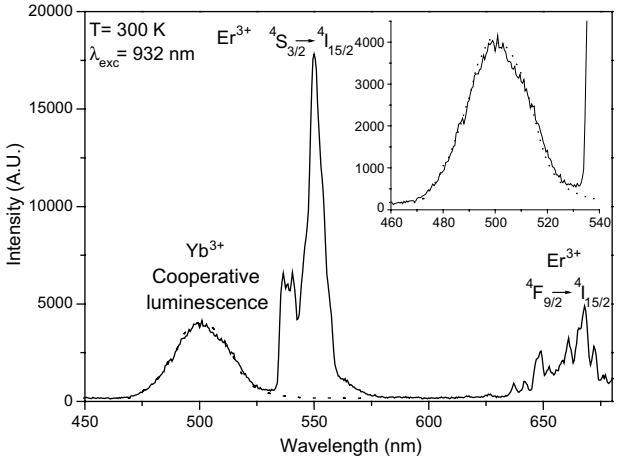

Fig. 7. Visible emission spectrum of $Li_6Y(BO_3)_3$:Yb 20% under diode excitation ($\lambda_{\text{exc}} = 932$ nm) at room temperature. Broken line: convolution product of infrared spectrum ($\lambda_{\text{exc}} = 932$ nm).

where G and F the visible and infrared spectra, respectively and $\bar{\nu}$ and $\bar{\nu}'$ the wave numbers in the infrared range.

The result fits with a good accordance the part of the spectrum between 465 nm and 530 nm (broken line in Fig. 7). The intensity of the cooperative blue emission, I_{coop}, is proportional to the square of the population of the excited state N_2. The lifetime τ_{coop} is then supposed to be half of the infrared value τ_{IR}.

$$I_{coop}(t) \propto \{N_2(t)\}^2 \propto \exp\left(-\frac{t}{\tau_{coop}}\right)$$

$$\text{with } N_2(t) \propto \exp\left(-\frac{t}{\tau_{IR}}\right) \text{ and } \tau_{coop} = \frac{\tau_{IR}}{2}$$

The lifetime of the emission at 500 nm was recorded for the 20% ytterbium doped-compound. Its value is equal to (498 ± 25) μs which is close to the expected value corresponding to the half of the infrared lifetime of the emission which is about to (1.19 ± 0.06) ms.

4. Conclusion

The energy level assignment has been successfully conducted on polycrystalline samples. The position of the barycenter plot deduced from the energy diagram is close to the semi-empiric line proposed by Antic-Fidancev which confirms our attribution. The lifetime study revealed the classical decrease when concentration increases. The radiative lifetime was found to be close to 1 ms. The evolution between the lifetimes measured at several emission wavelengths was attributed to a shorter lifetime for transitions issued from the highest excited Stark level (7). Finally, the study of the blue-green luminescence revealed that it is the result of two mechanisms: erbium emission at 550 nm after upconversion and cooperative luminescence of ytterbium ions.

Acknowledgement

This investigation was supported by the CNRS. Jean Sablayrolles thanks the CNRS and the Conseil Régional d'Aquitaine for fundings.

References

[1] S. Chénais, F. Druon, F. Balembois, G. Lucas-Leclin, P. Georges, A. Brun, M. Zavelani-Rossi, F. Augé, J.P. Chambaret, G. Aka, D. Vivien, Appl. Phys. B: Lasers Opt. 72 (2001) 389.
[2] C. Hönninger, R. Paschotta, M. Graf, F. Morier-Genoud, G. Zhang, M. Moser, S. Biswal, J. Nees, A. Braun, G.A. Mourou, I. Johannsen, A. Giesen, W. Seeber, U. Keller, Appl. Phys. B: Lasers Opt. 69 (1999) 3.
[3] Y. Zaouter, J. Didierjean, F. Balembois, G. Lucas-Leclin, F. Druon, P. Georges, J. Petit, P. Goldner, B. Viana, Opt. Lett. 31 (1) (2006) 119.
[4] F. Druon, F. Balembois, P. Georges, C.R. Phys. 8 (2) (2007) 153.
[5] J. Sablayrolles, V. Jubera, J.P. Chaminade, I. Manek-Hönninger, S. Murugan, T. Cardinal, R. Olazcuaga, A. Garcia, F. Salin, Opt. Mater. 27 (2005) 1681.
[6] A. Brenier, A. Yoshikawa, K. Lebbou, A. Jouini, O. Aloui-Lebbou, G. Boulon, T. Fukuda, J. Lumin. 126 (2) (2007) 547.
[7] M. Delaigue, V. Jubera, J. Sablayrolles, J.P. Chaminade, A. Garcia, I. Manek-Hönninger, Appl. Phys. B: Lasers Opt. 87 (4) (2007) 693.
[8] A. Ellens, H. Andres, M.L.H. ter Heerdt, R.T. Wegh, A. Meijerink, G. Blasse, Phys. Rev. B: Condens. Matter. Mater. Phys. 55 (1) (1997) 180.
[9] E. Antic-Fidancev, J. Alloys Compd. 300–301 (2000) 2.
[10] C. Tu, A. Jiang, Z. Luo, Jiegou Huaxue 8 (3) (1989) 215.
[11] Z. Luo, H. Zhang, Y.D. Huang, M.W. Qiu, Y.C. Huang, C.Y. Tu, A.D. Jiang, Cryst. Res. Technol. 26 (1) (1991) K5.
[12] Y. Huang, C. Tu, Z. Luo, G. Chen, Optic. Comm. 92 (1–2–3) (1992) 57.
[13] C. Tu, A. Jiang, Y. Huang, G. Chen, Z. Luo, Guisuanyan Xuebao 21 (6) (1993) 568.
[14] J. Holsa, M. Leskela, J. Lumin. 48–49 (2) (1991) 497.
[15] V. Jubera, J.P. Chaminade, A. Garcia, F. Guillen, C. Fouassier, J. Lumin. 101 (1-2) (2003) 1.
[16] R.P. Yavetskii, E.F. Dolzhenkova, M.F. Dubovik, T.I. Korshikova, A.V. Tolmachev, Crystallogr. Rep. 50 (1) (2005) S88.
[17] R.P. Yavetskiy, A.V. Tolmachev, E.F. Dolzhenkova, V.N. Baumer, J. Alloys Compd. 429 (1-2) (2007) 77.
[18] M.J. Knitel, P. Dorenbos, C.W.E. van Eijk, B. Plasteig, B. Viana, A. Kahn-Harari, D. Vivien, Nucl. Instrum. Meth. Phys. Res. Sect. A. 443 (2–3) (2000) 364.
[19] J.P. Chaminade, V. Jubera, A. Garcia, P. Gravereau, C. Fouassier, J. Optoelectron. Adv. Mater. 2 (5) (2000) 451.
[20] J.P. Chaminade, O. Viraphong, F. Guillen, C. Fouassier, B. Czirr, IEEE Trans. Nucl. Sci. 48 (4 Pt. 1) (2001) 1158.
[21] Y. Zhao, X. Gong, Y. Lin, Z. Luo, Y. Huang, Mater. Lett. 60 (3) (2006) 418.
[22] Y.W. Zhao, X.H. Gong, Y.J. Chen, L.X. Huang, Y.F. Lin, G. Zhang, Q.G. Tan, Z. Luo, Y.D. Huang, Appl. Phys. B: Lasers Opt. 88 (1) (2007) 51.
[23] J. Sablayrolles, V. Jubera, F. Guillen, A. Garcia, Spectrochimic. Acta, Part A, (2007), doi:10.1016/j.saa.2007.06.004.
[24] R.D. Shanon, C.T. Prewitt, Acta Cryst. B 25 (1969) 955.
[25] J. Hölsa, M. Leskalä, J. Lumin. 48–49 (1991) 497.
[26] V. Jubera, J.P. Chaminade, A. Garcia, F. Guillen, C. Fouassier, J. Lumin. 101 (2003) 1.
[27] G.K. Abdullaev, H.S. Mamedov, Kristallografiya (Crystal Reports) 22 (1977) 389.
[28] M. Kbala, A. Levasseur, C. Fouassier, P. Hagenmuller, Solid State Ionics 6 (1982) 191.
[29] A. Bensalah, Y. Guyot, M. Ito, A. Brenier, H. Sato, T. Fukuda, G. Boulon, Opt. Mater. 26 (2004) 375.
[30] R. Ternane, G. Boulon, Y. Guyot, M.T. Cohen-Adad, M. Trabelsi-Ayedi, N. Kbir-Ariguib, Opt. Mater. 22 (2003) 117.
[31] P.H. Haumesser, R. Gaumé, B. Viana, E. Antic-Fidancev, D. Vivien, J. Phys.: Condens. Matter. 13 (23) (2001) 5427.
[32] F. Auzel, G. Baldacchini, L. Laversenne, G. Boulon, Opt. Mater. 24 (2003) 103.
[33] E.A. Milne, J. London Math. Soc. 1 (1926) 40.
[34] T. Forster, Ann. Phys. (Leipz.) 2 (1948) 55.
[35] D.L. Dexter, J. Chem. Phys. 21 (1953) 836.
[36] D.E. McCumber, Phys. Rev., A: At. Mol., Opt. Phys. 136 (4) (1964) 954.
[37] C. Goutaudier, K. Lebbou, Y. Guyot, M. Ito, H. Canibano, A. El Hassouni, L. Laversenne, M.T. Cohen-Adad, G. Boulon, Ann. Chim. Sci. Mat. 28 (6) (2003) 73.
[38] M. Ito, C. Goutaudier, Y. Guyot, K. Lebbou, T. Fukuda, G. Boulon, J. Phys.: Condens. Matter. 16 (2004) 1501.
[39] G. Boulon, L. Laversenne, C. Goutaudier, Y. Guyot, M.T. Cohen-Adad, J. Lumin. 102–103 (2003) 417.
[40] P. Goldner, B. Schaudel, M. Prassas, Phys. Rev. B: Condens. Matter. Mater. Phys. 65 (5) (2002) 054103.
[41] E. Nakazawa, S. Shionoya, Phy. Rev. Lett. 25 (25) (1970) 1710.
[42] V.V. Ovsyankin, in: A.A. Kaplyanskii, R.M. MacFarlane (Eds.), Spectroscopy of Solids Containing Rare Earth Ions, Elsevier Science Publishers, Amsterdam, 1987, pp. 447–455, Chapter 7.